Available on the CERN CDS information server **CMS PAS SUS-12-016**

CMS Physics Analysis Summary

Contact: cms-pag-conveners-susy@cern.ch 2012/07/06

Search for supersymmetery in final states with missing transverse energy and 0, 1, 2, or $\geq$3 b jets in 8 TeV pp collisions

The CMS Collaboration

Abstract

A search for supersymmetry in the jets and missing transverse energy final state is performed in pp collisions at a centre of mass energy of at $\sqrt{s} = 8$ TeV. The data sample corresponds to an integrated luminosity of 3.9 fb^{-1} collected by the CMS experiment at the LHC. In this search, a kinematic variable, α_{T}, is used as the main discriminator between events with genuine and misreconstructed missing transverse energy. The search is performed in a signal region that is binned in the scalar sum of the transverse energy of jets and the number of jets identified to originate from a bottom quark. No excess of events over the standard model expectation is found. Exclusion limits are set in a simplified model of gluino pair production and decay to a final state of two top-antitop quark pairs and two neutralinos.

1 Introduction

Supersymmetry (SUSY) is generally regarded as one of the most likely extensions to the Standard Model of particle physics (SM) [1–8]. It is a well-establised theory based on the unique extension of the space-time symmetry group underpinning the SM, introducing a relationship between fermions and bosons. If the multiplicative quantum number R-parity is conserved [9], SUSY particles such as squarks and gluinos are produced in pairs and decay to the lightest SUSY particle (LSP), which is generally assumed to be a weakly interacting massive particle. Hence, a typical final-state signature is rich in jets and contains a significant amount of missing transverse energy ($\not\!\!E_{\mathrm{T}}$).

The search described below is therefore designed to be sensitive to missing transverse energy signatures in events with two or more energetic jets. These events are categorised according to the number of reconstructed jets originating from bottom quarks (b jets) per event. This approach improves the sensitivity to third-generation squark signatures while maintaining the ability to identify a wide variety of SUSY event topologies, which arise from the main production mechanisms of massive coloured sparticles at the LHC, namely squark-squark, squark-gluino and gluino-gluino pairs. This analysis follows closely that described in Ref. [10], which is in turn based on previous inclusive searches [11, 12]. The results presented here are based on a data sample of pp collisions collected in 2012 at a centre-of-mass energy of 8 TeV, which corresponds to an integrated luminosity of 3.9 fb^{-1}.

In 2010 and 2011 the CMS and ATLAS experiments performed various searches [11–19] for the production of massive coloured sparticles and their subsequent decay to a final state of jets and missing transverse energy. These searches were performed with a dataset of pp collisions at $\sqrt{s} = 7$ TeV, and no significant deviations from SM expectations were observed. The majority of these searches were interpreted in the context of a specific model of SUSY-breaking, the constrained minimal supersymmetric extension of the standard model (CMSSM) [20–22]. The simplifying assumption of universality at an energy scale of $\mathcal{O}(10^{16})$ GeV makes the CMSSM a useful framework to study SUSY phenomenology at colliders, and to benchmark the performance of experimental searches. However, these universality conditions result in significant restrictions on the possible SUSY particle mass spectra. For example, the CMSSM prevents the realisation of compressed mass spectra, where the mass difference between the initially produced squark or gluino and the LSP is small.

Alternatively, simplified models [23–26] can be used to interpret the search results presented below. Each model is characterised by a single production and decay mode involving a limited set of SUSY and SM particles. These models allow comprehensive studies of individual SUSY event topologies, which are performed in a two-dimensional parameter space of different sparticle masses and mass splittings. One such simplified model is used to interpret the result presented below, which is gluino pair production and decay to a final state of two top-antitop quark pairs and two neutralinos.

2 The CMS apparatus

The central feature of the CMS detector is a superconducting solenoid, which provides an axial magnetic field of 3.8 T. The bore of the solenoid is instrumented with several particle detection systems. Silicon pixel and strip tracking systems measure charged particle trajectories with full azimuthal (ϕ) coverage and a pseudorapidity acceptance of $|\eta| < 2.5$, where $\eta \equiv -\ln[\tan(\theta/2)]$ and θ is the polar angle with respect to the counterclockwise beam direction. The resolutions on the transverse momentum and impact parameter of a charged particle with $p_{\mathrm{T}} < 40\,\mathrm{GeV}$

is typically 1% and 15 μm, respectively. A lead tungstate crystal electromagnetic calorimeter (ECAL) and a brass/scintillator hadron calorimeter surround the tracking volume. The forward region is covered by an iron/quartz-fiber hadron calorimeter. The ECAL covers $|\eta| < 3.0$ and provides an energy resolution of better than 0.5% for unconverted photons with transverse energies above 100 GeV. The hadron calorimeters cover $|\eta| < 5.0$ with a resolution in jet energy, E (GeV), of about $100\%/\sqrt{\mathrm{E}}$. Muons are identified in gas-ionization detectors, covering $|\eta| < 2.4$, embedded in the steel return yoke. The CMS detector is nearly hermetic, which allows for momentum-balance measurements in the plane transverse to the beam axis. A detailed description of the CMS detector can be found elsewhere [27].

3 Object definition

The offline selection criteria and event reconstruction follows the procedure described in [11, 12]. Jets are reconstructed from energy deposits in the calorimeter towers, clustered by the anti-k_{T} algorithm [28] with a size parameter of 0.5. The raw jet energies measured by the calorimeter systems are corrected to remove the effects of overlapping pp collisions (pile-up) [29, 30], and to establish a uniform relative response in η and a calibrated absolute response in transverse momentum p_{T} [31]. Jets considered in the analysis are generally required to have transverse energy $E_{\mathrm{T}} > 50$ GeV. Events are vetoed if any additional jet satisfies both $E_{\mathrm{T}} > 50$ GeV and $|\eta| > 3$, or rare, spurious signals are identified in the calorimeters [32, 33]. The highest-E_{T} jet is required to be within the central tracker acceptance ($|\eta| < 2.5$) and the two highest-E_{T} jets must each have $E_{\mathrm{T}} > 100$ GeV. To suppress SM processes with genuine $\not\!\!E_{\mathrm{T}}$ from neutrinos, events containing an isolated electron [34] or muon [35] with $p_{\mathrm{T}} > 10$ GeV are vetoed. To select a pure multi-jet topology, events are vetoed in which an isolated photon [36] with $p_{\mathrm{T}} > 25$ GeV is found.

The presence of a b jet is identified through a vertex that is displaced with respect to the primary interaction, using the combined secondary vertex algorithm [37] which incorporates several variables related to the vertex to build a discriminator between jets originating from bottom quarks and other sources. These include jets from c quarks and light-flavour quarks. Discriminator values above a certain threshold are used to tag jets as reconstructed b jets. This threshold is chosen such that the mis-tagging rate, i.e. the probability to tag jets originating from light-flavour quarks as b jets, is approximately 1% for jets with a transverse momenta of 100 GeV [37, 38]. This typically results in a b tagging efficiency, i.e. the probability to correctly tag jets originating from b quarks, in the range $60 - 70\%$ [37, 38].

The following two variables characterize the visible energy and missing momentum in the transverse plane: the scalar sum of the transverse energy E_{T} of jets, defined as $H_{\mathrm{T}} = \sum_{i=1}^{N_{\mathrm{jet}}} E_{\mathrm{T}}$, and the magnitude of the vector sum of the transverse momenta $\vec{p}_{\mathrm{T}}$ of jets, defined as $\not\!\!H_{\mathrm{T}} = |\sum_{i=1}^{N_{\mathrm{jet}}} \vec{p}_{\mathrm{T}}|$, where N_{jet} is the number of jets with $E_{\mathrm{T}} > 50$ GeV. Significant hadronic activity in the event is ensured by requiring $H_{\mathrm{T}} > 275$ GeV. Following these selections, the background from multi-jet production, a manifestation of quantum chromodynamics (QCD), is still several orders of magnitude larger than the typical signal expected from SUSY.

4 Selection of multi-jet events with missing transverse energy

The α_{T} kinematic variable, first introduced in Refs. [39–41], is used in the selection of multi-jet events to efficiently reject events either without significant $\not\!\!E_{\mathrm{T}}$ or with transverse energy mismeasurements, whilst retaining a large sensitivity to new physics with genuine $\not\!\!E_{\mathrm{T}}$ signatures.

For dijet events, the α_T variable is defined as:

$$\alpha_T = \frac{{E_T}^{j_2}}{M_T} \quad , \quad M_T = \sqrt{\left(\sum_{i=1}^{2} {E_T}^{j_i}\right)^2 - \left(\sum_{i=1}^{2} p_x^{j_i}\right)^2 - \left(\sum_{i=1}^{2} p_y^{j_i}\right)^2}. \tag{1}$$

where ${E_T}^{j_2}$ is the transverse energy of the least energetic jet of the two, and M_T is the transverse mass of the dijet system. For a perfectly measured dijet event with ${E_T}^{j_1} = {E_T}^{j_2}$ and jets back-to-back in ϕ, and in the limit of large jet momenta compared to their masses, the value of α_T is 0.5. In the case of an imbalance in the measured transverse energies of back-to-back jets, α_T is smaller than 0.5. Values significantly greater than 0.5 are observed when the two jets are not back-to-back, recoiling against genuine $\not\!\!E_T$.

For events with three or more jets, an equivalent dijet system is formed by combining the jets in the event into two pseudo-jets. The E_T of each of the two pseudo-jets is calculated as the scalar sum of the measured E_T of the contributing jets. The combination chosen is the one that minimizes the E_T difference (ΔH_T) between the two pseudo-jets. This simple clustering criterion provides the best separation between multi-jet events and events with genuine $\not\!\!E_T$.

Events with extremely rare but large stochastic fluctuations in calorimetric measurements of jet energies can lead to values of α_T slightly above 0.5. Such events are rejected by requiring $\alpha_T > 0.55$. A similar behaviour is observed in events with reconstruction failures, severe energy losses due to detector inefficiencies, or jets below the E_T threshold that result in significant $\not\!\!H_T$ relative to the value of $\not\!\!E_T$ (as measured by the calorimeter systems, which is not affected by jet E_T thresholds). These classes of events are rejected by applying dedicated vetoes, described further in Ref. [12]. The leakage above 0.5 becomes smaller with increasing H_T. This is due in part to increasing average jet energy and thus improving jet energy resolution. Further, the relative impact of jets falling below the E_T threshold is reduced as the scale of the event (i.e. H_T) increases.

The signal region is defined by $H_T > 275\,\text{GeV}$ and $\alpha_T > 0.55$, which is divided into eight bins in H_T: two bins of width 50 GeV in the range $275 < H_T < 375\,\text{GeV}$, five bins of width 100 GeV in the range $375 < H_T < 875\,\text{GeV}$, and a final open bin, $H_T > 875\,\text{GeV}$. As in Ref. [12], the jet E_T threshold is scaled down to 37 GeV and 43 GeV for the regions $275 < H_T < 325\,\text{GeV}$ and $325 < H_T < 375\,\text{GeV}$, respectively. The highest-E_T jet threshold is also scaled accordingly. This is done in order to maintain a background composition and event kinematics similar to those observed for the higher H_T bins. Candidate events are further categorised according to whether they contain exactly zero, one, two, or at least three reconstructed b jets.

Events in the signal sample are recorded with multiple trigger conditions that must satisfy requirements on both H_T and α_T in the range ($H_T > 250\,\text{GeV}$ and $\alpha_T > 0.55$) to ($H_T > 400\,\text{GeV}$ and $\alpha_T > 0.51$). The trigger efficiency is defined as the probability with which events that satisfy the signal sample selection criteria also satisfy the trigger conditions, which is measured from data to be $89.6 \pm 0.6\,\%$ and at least $98.5 \pm 0.5\,\%$ for the regions $275 < H_T < 325\,\text{GeV}$ and $H_T > 325\,\text{GeV}$, respectively.

A disjoint hadronic control sample consisting predominantly of multi-jet events is defined by inverting the α_T requirement for a given H_T region, which is used primarily in the estimation of any residual background from multi-jet events. These events are recorded by a set of H_T trigger conditions.

5 Background estimation from data

Once all selection requirements have been imposed, the contribution from multi-jet events is expected to be negligible. The remaining significant backgrounds in the hadronic signal region stem from SM processes with genuine $\not{E}_T$ in the final state. In the case of events where no b jets are identified, the largest backgrounds with genuine $\not{E}_T$ arise from the production of W and Z bosons in association with jets. The weak decay $Z \to \nu\bar{\nu}$ is the only relevant contribution from Z + jets events. For W + jets events, the two relevant sources are leptonic W decays, in which the lepton is not reconstructed or fails the isolation or acceptance requirements, and the weak decay $W \to \tau\nu$ where the τ decays hadronically and is identified as a jet. For events with one or more reconstructed b jets however, top quark production followed by semi-leptonic weak decays becomes the most important single background source. For events with only one reconstructed b jet, the contribution of both W + jets and Z + jets backgrounds are of a similar size to the top background. For events with two reconstructed b jets, $t\bar{t}$ production dominates, whilst events with three or more reconstructed b jets originate almost exclusively from $t\bar{t}$ events, in which one or several jets are misidentified as b jets.

In order to estimate the contributions from each of these backgrounds, three data control samples are used, which are binned in the same way as the signal sample. A μ + jets data sample provides an estimate of the contributions from top quark and W production leading to W + jets final states. The remaining irreducible background of $Z \to \nu\bar{\nu}$ + jets events in the hadronic signal region is estimated from both a data sample of $Z \to \mu\mu$ + jets and γ + jets events, which share kinematic properties but have different acceptances. The $Z \to \mu\mu$ + jets events have identical kinematic properties when the two muons are ignored, but a smaller branching ratio, while the γ + jets events have similar kinematic properties when the photon is ignored [42, 43], but a larger production cross section. The event selection criteria for the control samples are defined to ensure that any potential contamination from multi-jet events is negligible. Further, the selection also suppress signal contamination from a wide variety of SUSY models, including those considered in this analysis, to a negligible level.

5.1 Definition of data control samples

The μ + jets sample is recorded using a trigger strategy which requires an isolated muon above a p_T threshold of 24 GeV and within $|\eta| < 2.1$. The event selection requires exactly one isolated muon that satisfies stringent quality criteria, with $p_T > 30$ GeV and $|\eta| < 2.1$, in order for the trigger to be maximally efficient, around 88.0 ± 2.0 %.

The transverse mass of the muon and $\not{E}_T$ system must be larger than 30 GeV to ensure a sample rich in W bosons. The muon is required to be separated from the closest jet in the event by $\Delta\eta$ and $\Delta\phi$ such that the distance $\Delta R \equiv \sqrt{\Delta\eta^2 + \Delta\phi^2} > 0.5$. Further, the event is rejected if a second muon candidate is identified that does not satisfy all quality criteria or is non-isolated or is outside acceptance, and the two muon candidates have an invariant mass that is within a window of ± 25 GeV around the mass of the Z boson. The requirement $\alpha_T > 0.55$ is imposed when zero b jets are reconstructed per event; for all other event categories, in which at least one b jet is reconstructed, no α_T requirement is used [10].

The $\mu\mu$ + jets sample follows the same trigger strategy and muon identification criteria as the μ + jets sample, except that in the event selection criteria, the threshold for the muon with the lower p_T is 10 GeV. This leads to a trigger efficiency of 95 ± 2% rising to 98 ± 2% with increasing H_T. The event selection requires exactly two oppositely charged, isolated muons satisfying stringent quality criteria, and an invariant mass within a window of ± 25 GeV around the mass of the Z boson. Both muons are required to be separated from their closest jets in the event by

the distance $\Delta R > 0.5$.

The γ + jets sample is selected using a dedicated photon trigger condition requiring a localized, large energy deposit in the ECAL with $E_T > 150\,\text{GeV}$ that satisfies loose photon identification and isolation criteria [36]. The offline selection requires $H_T > 375\,\text{GeV}$, $\alpha_T > 0.55$, and a single photon to be reconstructed with $E_T > 165\,\text{GeV}$, $|\eta| < 1.45$, satisfying tight isolation criteria, and with a minimum distance to any jet of $\Delta R > 1.0$. For these selection criteria, the photon trigger condition is found to be fully efficient.

5.2 Method for estimating genuine E_T background

The method used to estimate the background contributions in the hadronic signal region relies on the use of translation factors, which are constructed per bin in the two dimensions of H_T and number of reconstructed b jets per event, n_b^{reco}. Each factor, determined from simulation, is defined as the ratio of yields in a given bin of the hadronic signal sample (N_{MC}^{signal}) and corresponding bin of the control sample ($N_{MC}^{control}$). The factors are used to translate the observed yield measured in a control sample bin ($N_{obs}^{control}$) into an expectation for the yield in the corresponding bin of the hadronic signal sample (N_{pred}^{signal}):

$$N_{pred}^{signal}(H_T, n_b^{reco}) = N_{obs}^{control}(H_T, n_b^{reco}) \times \frac{N_{MC}^{signal}}{N_{MC}^{control}}(H_T, n_b^{reco}). \quad (2)$$

The number of reconstructed b jets per event (n_b^{reco}) is estimated from a method based on truth-level information contained in the simulation, namely: the numbers of jets originating from underlying b quarks, n_b, and from light quarks, n_q, per event. All relevant combinations of n_b and n_q are considered, and event counts are recorded in bins of H_T for each combination, $N(n_b, n_q)$. The b tagging efficiency, ϵ, and a flavour-averaged mistagging rate, m, are measured also from simulation for each H_T bin, with both quantities averaged over jet p_T and η. Corrections are applied to both ϵ and m in order to match the corresponding measurements with data [37, 38]. The aforementioned information is sufficient to determine an accurate prediction for n_b^{reco}. For example, an estimate for the number of events with zero reconstructed b jets is given by the expression:

$$n_0^{reco} = \sum_{n_b \geq 0,\, n_q \geq 0} N(n_b, n_q) \times (1-\epsilon)^{n_b} \times (1-m)^{n_q} \quad (3)$$

A similar treatment is used for the other b jet multiplicity categories. The yields from simulation, binned according to H_T and n_b^{reco} as determined with the method described above, are found to be in good agreement with the yields obtained directly from the simulation. The method exploits the ability to make precise measurements of $N(n_b, n_q)$, ϵ and particularly m, which means that predicted event yields for a given b jet category can be made with a higher statistical precision than obtained directly from simulation. This is particularly important for events with $n_b^{reco} \geq 3$, which requires the presence of mistagged jets in the event. In this case, the most probable (albeit small) background is $t\bar{t}$, with two correctly tagged b jets and an additional mistagged jet.

Any mismodelling in the simulation of the event kinematics or instrumental effects observed in data are expected to largely cancel in the ratio of yields used to construct the translation factors, given that the data control and signal samples, and the corresponding event samples from simulation, are defined to be kinematically similar. However, a systematic uncertainty

is assigned to each translation factor to account for theoretical uncertainties [43] and residual biases in the simulation modelling [11]. The magnitudes of the systematic uncertainties are determined from a representative set of closure tests in data, in which yields from one of the three indepedent control samples, along with the corresponding translation factors obtained from simulation, are used to predict the yields in another control sample, following the same prescription defined in Equation 2. The contamination from multi-jet events and any potential signal is expected to be negligible. Therefore, the closure tests carried out between control samples probe the properties of the relevant SM backgrounds.

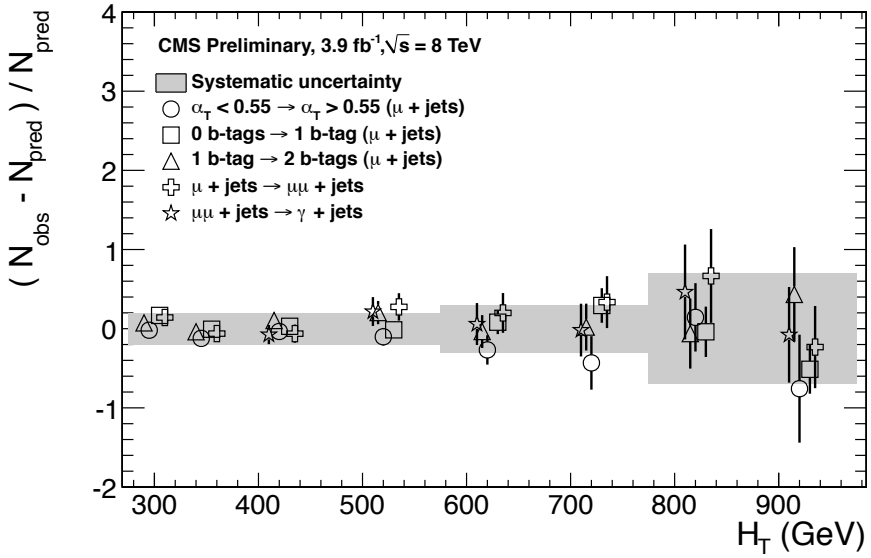

Figure 1: A set of closure tests overlaid on top of grey bands that represent the systematic uncertainties used for the three H_{T} regions in the final simultaneous fit.

A set of five closure tests, which probe key ingredients of the simulation modelling that may introduce biases to the translation factors, and the H_{T}-dependent systematic uncertainties are shown in Fig. 1. The first three closure tests are carried out within the μ + jets sample, and probe the modelling of the α_{T} distribution in genuine $\not\!\!E_{\mathrm{T}}$ events (circles), the relative composition between W + jets and top events (squares), and the modelling of the reconstruction of b jets (triangles), respectively. The fourth test (crosses), connecting the μ + jets and $\mu\mu$ + jets control samples, addresses the modelling of the relative contributions of Z + jets to W + jets and top events while the fifth test (stars) deals with the consistency between the Z$\rightarrow \mu\mu$ + jets and γ + jets samples.

All individual closure tests demonstrate, within the statistical precision of each test, that there are no significant biases inherent in the translation factors obtained from simulation. The level of closure achieved in these tests is used to determine systematic uncertainties that are assigned to the translation factors. For each of the three regions $275 < H_{\mathrm{T}} < 575\,\mathrm{GeV}$, $575 < H_{\mathrm{T}} < 775\,\mathrm{GeV}$ and $H_{\mathrm{T}} > 775\,\mathrm{GeV}$, the systematic uncertainties are defined such that at least 90% of the closure test points in each H_{T} region are covered. This conservative procedure yields values of 20%, 30% and 70% for the three H_{T} regions defined above. Uncertainties related to the modelling of b jets in simulation are found to be negligible in comparison to the aforementioned uncertainties after corrections are applied to the efficiency and mis-tagging rates of b jets obtained from simulation, in order to account for residual differences with respect to measurements in data.

6 Results and interpretation

A binned likelihood fit using all four data samples is carried out to obtain a consistent prediction of the SM background:

$$L_{\text{total}} = L_{\text{hadronic}} \times L_{\mu+\text{jets}} \times L_{\mu\mu+\text{jets}} \times L_{\gamma+\text{jets}} \quad n_b < 3 \tag{4}$$

$$L_{\text{total}} = L_{\text{hadronic}} \times L_{\mu+\text{jets}} \quad n_b \geq 3 \tag{5}$$

The fit maximizes the total likelihood simultaneously in eight bins of H_{T} for each of the four categories of b tag multiplicity. L_{hadronic} describes the H_{T}-binned observations in the hadronic sample, while the terms $L_{\mu+\text{jets}}$, $L_{\mu\mu+\text{jets}}$, and $L_{\gamma+\text{jets}}$ describe the H_{T} binned yields in the μ + jets , $\mu\mu$ + jets, and γ + jets samples respectively. For each bin, the expected yields in the control samples are related to the components of the SM expectations in the hadronic signal sample via translation factors from simulation. Since for $n_b \geq 3$ the only relevant SM background arises from top events, only the μ+jets control sample is used in the likelihood to determine the background in the hadronic signal region for this b jet multiplicity. However, the translation factors account also for any possible (residual) contributions from W + jets, $\text{Z} \to \nu\bar{\nu}$ + jets, and other relevant SM backgrounds. Three nuisance parameters per data control sample are used to accommodate the H_{T}-dependent systematic uncertainties on the translation factors. In addition, any potential contribution from the multi-jet background in the hadronic sample is estimated by exploiting the H_{T} dependence of the ratio of events that result in a value of α_{T} above and below some threshold value. This dependence on H_{T} is modelled as a falling exponential function, $A\text{e}^{-k\,H_{\text{T}}}$ [12]. The parameters A and k are the normalisation and exponential decay constants, respectively. Values of A and k are determined by the fit independently for each category of reconstructed b jets. The value of k is constrained via measurements in a multi-jet−enriched data side-band satisfying the criteria $H_{\text{T}} < 575\,\text{GeV}$ and $0.52 < \alpha_{\text{T}} < 0.55$. A further side band, defined by inverting the $\not{H}_{\text{T}}/\not{E}_{\text{T}}$ cleaning cut [12], is used to confirm that this method provides an unbiased estimator for k and to estimate a systematic uncertainty.

In order to test the compatibility of the observed yields with the expectations from SM processes only, the likelihood function is maximized over all fit parameters. A comparison of the observed yields and the SM expectations in bins of H_{T} for events with exactly zero, one, two, and at least three reconstructed b jets are shown in Figures 2, 3, 4 and 5, respectively, for the hadronic signal region, and the three control samples. For all four b jet categories, no significant excess above the SM expectation is observed in the hadronic signal region, and the control samples are well described by the SM hypothesis.

Limits are set in a simplified model of gluino pair production, where each gluino decays to two top quarks and a neutralino, leading to a four-top final state: $\text{pp} \to \tilde{\text{g}}\tilde{\text{g}} \to \text{t}\bar{\text{t}}\tilde{\chi}^0\text{t}\bar{\text{t}}\tilde{\chi}^0$. Figure 6 shows the upper limit at 95% CL on the cross section as a function of $m_{\tilde{\text{g}}}$ and m_{LSP}. Experimental uncertainties on the SM background predictions ($20-70\%$), the luminosity measurement (4.4%), and the total acceptance times efficiency of the selection for the signal model (13%) are included in the calculation of the limit. Any potential signal contamination in the control samples has been accounted for.

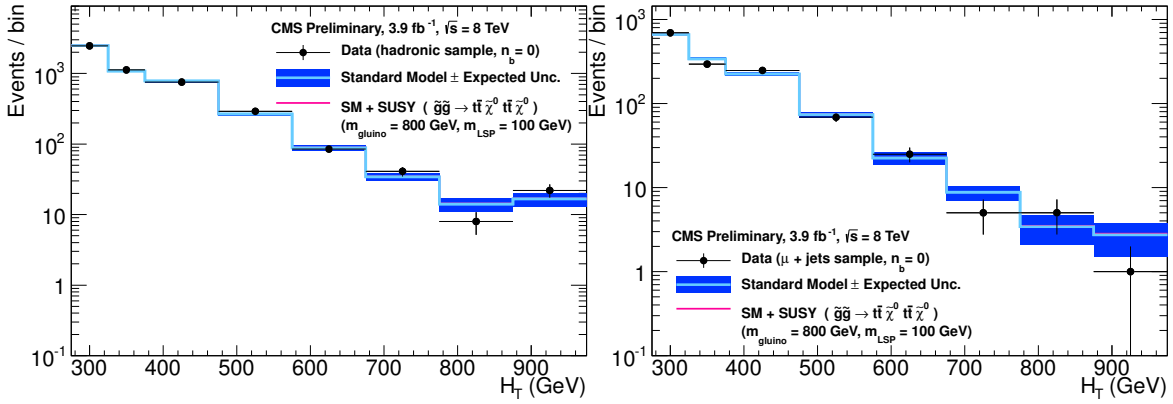

(a) Hadronic sample

(b) μ + jets sample

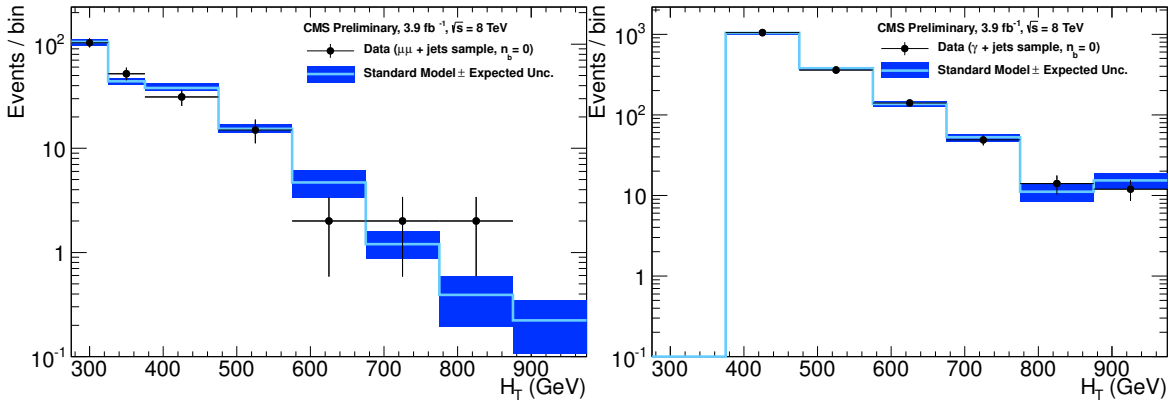

(c) $\mu\mu$ + jets sample

(d) γ + jets sample

Figure 2: Comparison of the observed yields and SM expectations given by the simultaneous fit in bins of H_T for the (a) hadronic, (b) μ + jets, (c) $\mu\mu$ + jets and (d) γ + jets samples when requiring exactly zero reconstructed b-jets. The event selection criteria for all three data control samples include the requirement $\alpha_T > 0.55$. The observed event yields in data (black dots) and the expectations and their uncertainties, as determined by the simultaneous fit, for all SM processes (light blue solid line with dark blue bands) are shown. For illustrative purposes only, the expected yields from pair produced gluinos ($m_{\text{gluino}} = 800\,\text{GeV}$), each decaying to a top-antitop quark pair and a neutralino ($m_{\text{LSP}} = 100\,\text{GeV}$), are superimposed on top of the SM expectation (magenta solid line).

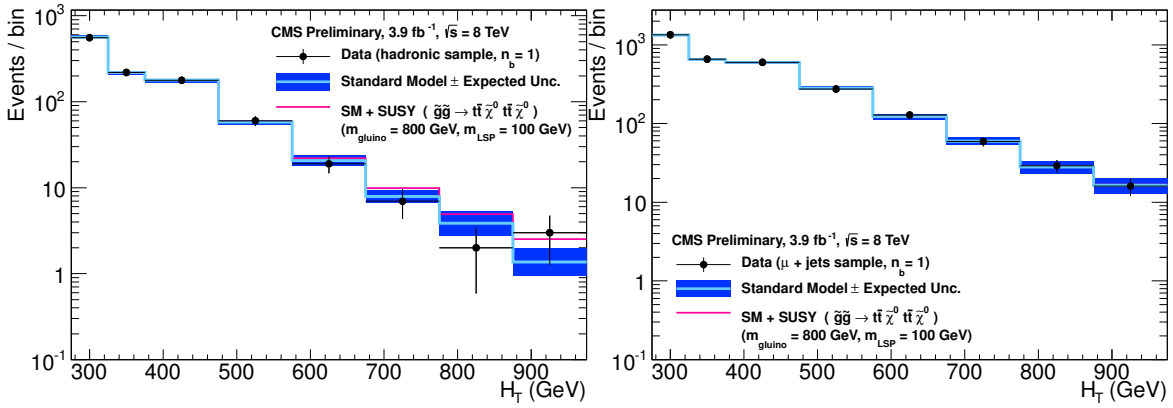

(a) Hadronic sample

(b) μ + jets sample

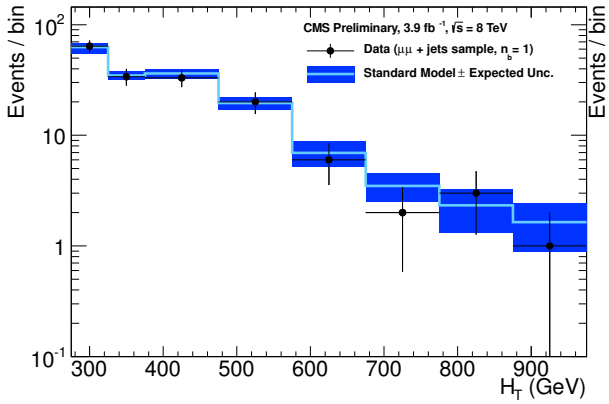

(c) $\mu\mu$ + jets sample

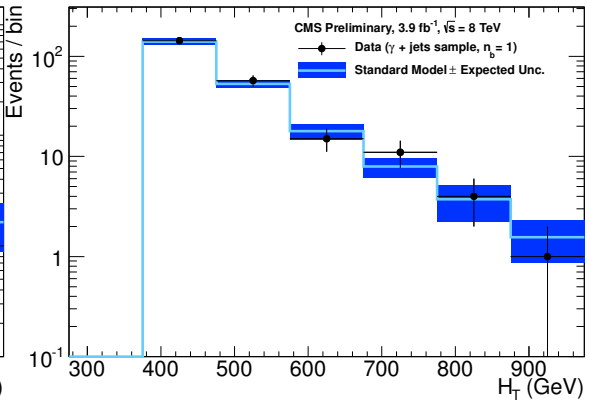

(d) γ + jets sample

Figure 3: Comparison of the observed yields and SM expectations given by the simultaneous fit in bins of H_T for the (a) hadronic, (b) μ + jets, (c) $\mu\mu$ + jets and (d) γ + jets samples when requiring exactly one reconstructed b-jet. The event selection criteria for the two muon data control samples do not include any requirement on α_T. The observed event yields in data (black dots) and the expectations and their uncertainties, as determined by the simultaneous fit, for all SM processes (light blue solid line with dark blue bands) are shown. For illustrative purposes only, the expected yields from pair produced gluinos ($m_{\text{gluino}} = 800\,\text{GeV}$), each decaying to a top-antitop quark pair and a neutralino ($m_{\text{LSP}} = 100\,\text{GeV}$), are superimposed on top of the SM expectation (magenta solid line).

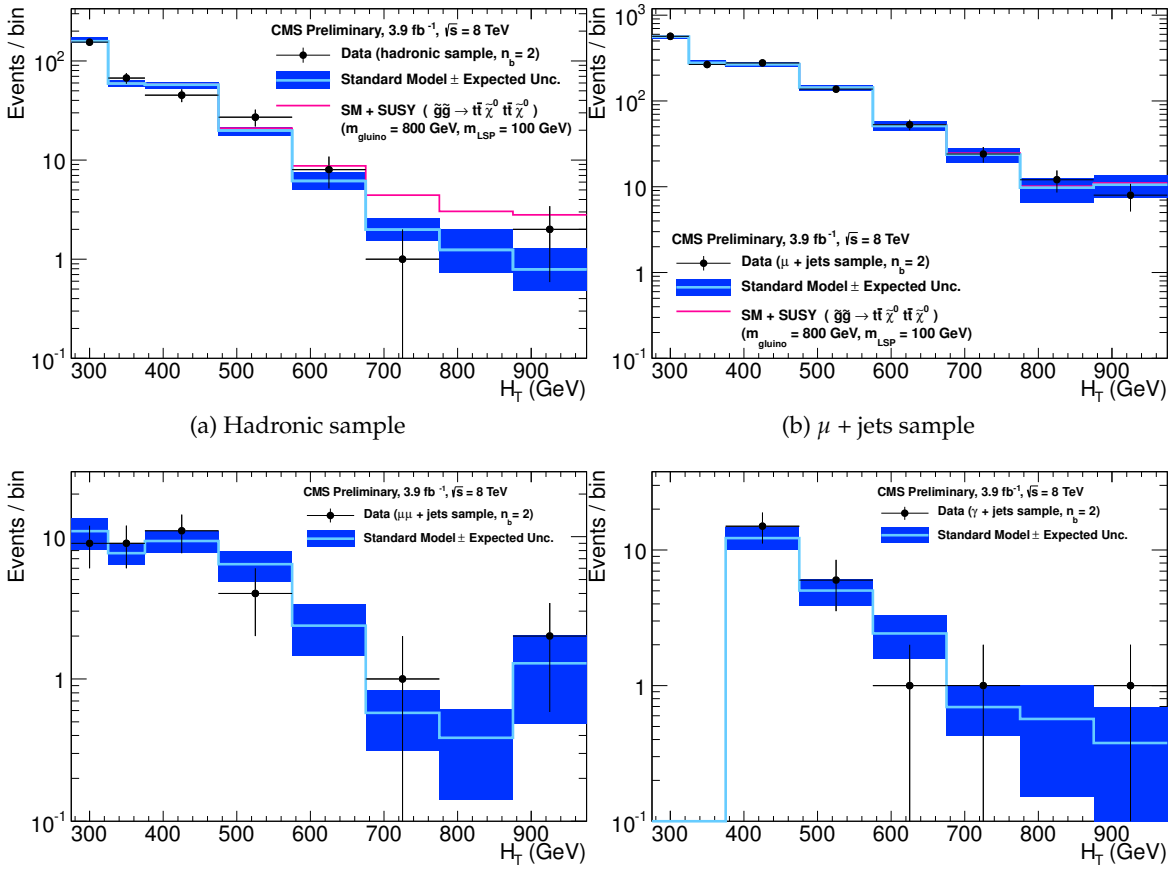

(a) Hadronic sample

(b) μ + jets sample

(c) $\mu\mu$ + jets sample

(d) γ + jets sample

Figure 4: Comparison of the observed yields and SM expectations given by the simultaneous fit in bins of H_T for the (a) hadronic, (b) μ + jets, (c) $\mu\mu$ + jets and (d) γ + jets samples when requiring exactly two reconstructed b-jets. The event selection criteria for the two muon data control samples do not include any requirement on α_T. The observed event yields in data (black dots) and the expectations and their uncertainties, as determined by the simultaneous fit, for all SM processes (light blue solid line with dark blue bands) are shown. For illustrative purposes only, the expected yields from pair produced gluinos ($m_{\text{gluino}} = 800\,\text{GeV}$), each decaying to a top-antitop quark pair and a neutralino ($m_{\text{LSP}} = 100\,\text{GeV}$), are superimposed on top of the SM expectation (magenta solid line).

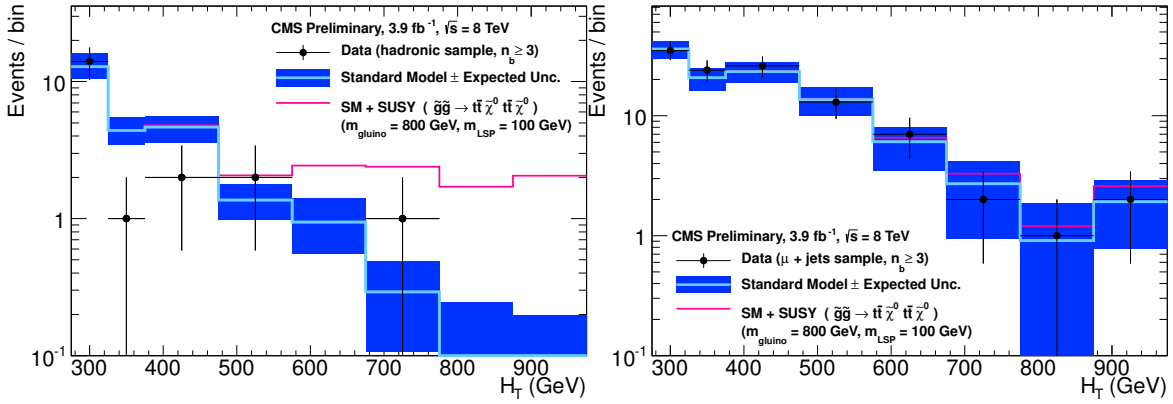

(a) Hadronic sample (b) μ + jets sample

Figure 5: Comparison of the observed yields and SM expectations given by the simultaneous fit in bins of H_T for the (a) hadronic and (b) μ + jets samples when requiring at least three reconstructed b-jets. The event selection criteria for the μ + jets data control sample does not include any requirement on α_T. The observed event yields in data (black dots) and the expectations and their uncertainties, as determined by the simultaneous fit, for all SM processes (light blue solid line with dark blue bands) are shown. For illustrative purposes only, the expected yields from pair produced gluinos ($m_{\text{gluino}} = 800\,\text{GeV}$), each decaying to a top-antitop quark pair and a neutralino ($m_{\text{LSP}} = 100\,\text{GeV}$), are superimposed on top of the SM expectation (magenta solid line).

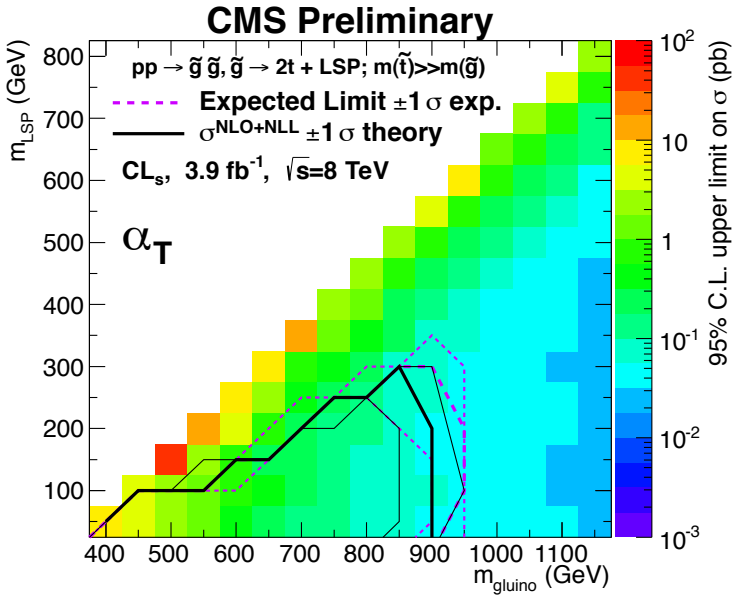

Figure 6: Upper limit on cross section at 95% CL as a function of $m_{\tilde{g}}$ and m_{LSP} for gluino pair production, with each gluino decaying to a top-antitop pair and a neutralino: $pp \to \tilde{g}\tilde{g} \to t\bar{t}\tilde{\chi}^0 t\bar{t}\tilde{\chi}^0$. The solid thick black line indicates the observed exclusion region assuming NLO+NLL SUSY production cross section. The thin black lines represent the observed excluded region when varying the cross section by its theoretical uncertainty. The dashed purple lines indicate the median (thick line) $\pm 1\sigma$ (thin lines) expected exclusion regions.

7 Summary

In summary, a search for supersymmetry based on a data sample of pp collisions collected at $\sqrt{s} = 8\,\text{TeV}$, corresponding to an integrated luminosity of 3.9 fb^{-1}, has been reported. Final states with two or more jets and significant $\not\!\!E_{\text{T}}$, as expected from high-mass squark and gluino production and decays, have been analysed. An exclusive search has been performed in a binned signal region defined by the scalar sum of the transverse energy of jets, H_{T}, and the number of jets identified to originate from a bottom quark. The sum of standard model backgrounds per bin has been estimated from a simultaneous binned likelihood fit to hadronic, μ + jets, $\mu\mu$ + jets, and γ + jets samples. The observed yields are found to be in agreement with the expected contributions from standard model processes and limits on a simplified model of gluino pair production and decay to two top-antitop quark pairs and two neutralinos have been set. In this simplified model, gluino masses below 850 GeV are excluded at 95% CL for a neutralino mass of 50 GeV. No limit can be set for neutralino masses above approximately 250 GeV.

References

[1] Y. A. Gol'fand and E. P. Likhtman, "Extension of the Algebra of Poincaré Group Generators and Violation of p Invariance", *JETP Lett.* **13** (1971) 323.

[2] J. Wess and B. Zumino, "Supergauge transformations in four dimensions", *Nucl. Phys. B* **70** (1974) 39, doi:10.1016/0550-3213(74)90355-1.

[3] H. P. Nilles, "Supersymmetry, Supergravity and Particle Physics", *Phys. Reports* **110** (1984) 1, doi:10.1016/0370-1573(84)90008-5.

[4] H. Haber and G. Kane, "The Search for Supersymmetry: Probing Physics Beyond the Standard Model", *Phys. Reports* **117** (1987) 75, doi:10.1016/0370-1573(85)90051-1.

[5] R. Barbieri, S. Ferrara, and C. A. Savoy, "Gauge Models with Spontaneously Broken Local Supersymmetry", *Phys. Lett. B* **119** (1982) 343, doi:10.1016/0370-2693(82)90685-2.

[6] S. Dawson, E. Eichten, and C. Quigg, "Search for Supersymmetric Particles in Hadron - Hadron Collisions", *Phys. Rev. D* **31** (1985) 1581, doi:10.1103/PhysRevD.31.1581.

[7] E. Witten, "Dynamical Breaking of Supersymmetry", *Nucl. Phys. B* **188** (1981) 513, doi:10.1016/0550-3213(81)90006-7.

[8] S. Dimopoulos and H. Georgi, "Softly Broken Supersymmetry and SU(5)", *Nucl. Phys. B* **193** (1981) 150, doi:10.1016/0550-3213(81)90522-8.

[9] G. R. Farrar and P. Fayet, "Phenomenology of the Production, Decay, and Detection of New Hadronic States Associated with Supersymmetry", *Phys. Lett. B* **76** (1978) 575, doi:10.1016/0370-2693(78)90858-4.

[10] CMS Collaboration, "Search for supersymmetery in final states with missing transverse energy and 0, 1, 2, or $\geq$3 b jets in 7 TeV pp collisions", CMS Physics Analysis Summary SUS-11-022, (2012).

[11] CMS Collaboration, "Search for Supersymmetry at the LHC in Events with Jets and Missing Transverse Energy", *Phys. Rev. Lett.* **107** (Nov, 2011) 221804, doi:10.1103/PhysRevLett.107.221804.

[12] CMS Collaboration, "Search for Supersymmetry in pp Collisions at 7 TeV in Events with Jets and Missing Transverse Energy", *Phys. Lett.* **B698** (2011) 196–218, doi:10.1016/j.physletb.2011.03.021, arXiv:1101.1628.

[13] CMS Collaboration, "Search for new physics with jets and missing transverse momentum in pp collisions at $\sqrt{s} = 7$ TeV", *JHEP* **2011** (2011) 1–46. 10.1007/JHEP08(2011)155.

[14] CMS Collaboration, "Inclusive search for squarks and gluinos in pp collisions at $\sqrt{s} = 7$ TeV", *Phys. Rev. D* **85** (Jan, 2012) 012004, doi:10.1103/PhysRevD.85.012004.

[15] CMS Collaboration, "Search for supersymmetry in events with b jets and missing transverse momentum at the LHC", *JHEP* **2011** (2011) 1–26. 10.1007/JHEP07(2011)113.

[16] ATLAS Collaboration, "Search for squarks and gluinos using final states with jets and missing transverse momentum with the ATLAS detector in proton-proton collisions", *Physics Letters B* **710** (2012), no. 1, 67 – 85, doi:10.1016/j.physletb.2012.02.051.

[17] ATLAS Collaboration, "Search for new phenomena in final states with large jet multiplicities and missing transverse momentum using $\sqrt{s}$ = 7 TeV pp collisions with the ATLAS detector", *JHEP* **2011** (2011) 1–38. 10.1007/JHEP11(2011)099.

[18] ATLAS Collaboration, "Search for Scalar Bottom Quark Pair Production with the ATLAS Detector in pp Collisions at $\sqrt{s}$ = 7 TeV", *Phys. Rev. Lett.* **108** (May, 2012) 181802, doi:10.1103/PhysRevLett.108.181802.

[19] ATLAS Collaboration, "Search for squarks and gluinos using final states with jets and missing transverse momentum with the ATLAS detector in proton-proton collisions", *Physics Letters B* **701** (2011), no. 2, 186 – 203, doi:10.1016/j.physletb.2011.05.061.

[20] A. H. Chamseddine, R. Arnowitt, and P. Nath, "Locally Supersymmetric Grand Unification", *Phys. Rev. Lett.* **49** (1982) 970, doi:10.1103/PhysRevLett.49.970.

[21] R. Arnowitt and P. Nath, "Supersymmetric mass spectrum in SU(5) supergravity grand unification", *Phys. Rev. Lett.* **69** (1992) 725, doi:10.1103/PhysRevLett.69.725.

[22] G. L. Kane et al., "Study of constrained minimal supersymmetry", *Phys. Rev. D* **49** (1994) 6173, doi:10.1103/PhysRevD.49.6173.

[23] J. Alwall, P. Schuster, and N. Toro, "Simplified Models for a First Characterization of New Physics at the LHC", *Phys. Rev.* **D79** (2009) 075020, doi:10.1103/PhysRevD.79.075020, arXiv:0810.3921.

[24] J. Alwall, M.-P. Le, M. Lisanti et al., "Model-Independent Jets plus Missing Energy Searches", *Phys.Rev.* **D79** (2009) 015005, doi:10.1103/PhysRevD.79.015005, arXiv:0809.3264.

[25] D. Alves, N. Arkani-Hamed, S. Arora et al., "Simplified Models for LHC New Physics Searches", arXiv:1105.2838. Official summary of results from the 'Topologies for Early LHC Searches' workshop, SLAC, September 2010.

[26] CMS Collaboration, "Interpretation of Searches for Supersymmetry", CMS Physics Analysis Summary SUS-11-016, (2012).

[27] CMS Collaboration, "The CMS experiment at the CERN LHC", *JINST* **03** (2008) S08004, doi:10.1088/1748-0221/3/08/S08004.

[28] M. Cacciari, G. P. Salam, and G. Soyez, "The anti-k_T jet clustering algorithm", *JHEP* **04** (2008) 063, doi:10.1088/1126-6708/2008/04/063.

[29] M. Cacciari and G. P. Salam, "Pileup subtraction using jet areas", *Physics Letters B* **659** (2008) 119 – 126, doi:10.1016/j.physletb.2007.09.077.

[30] M. Cacciari, G. P. Salam, and G. Soyez, "The catchment area of jets", *Journal of High Energy Physics* **2008** (2008), no. 04, 005.

[31] CMS Collaboration, "Determination of Jet Energy Calibration and Transverse Momentum Resolution in CMS", *JINST* **6** (2011) P11002, doi:10.1088/1748-0221/6/11/P11002, arXiv:1107.4277.

[32] CMS Collaboration, "Identification and filtering of uncharacteristic noise in the CMS hadron calorimeter", *JINST* **5** (2010) T03014, doi:10.1088/1748-0221/5/03/T03014.

[33] CMS Collaboration, "Electromagnetic calorimeter commissioning and first results with 7 TeV data", CMS Note CMS-NOTE-2010-012, (2010).

[34] CMS Collaboration, "Electron reconstruction and identification at $\sqrt{s} = 7$ TeV", CMS Physics Analysis Summary EGM-10-004, (2010).

[35] CMS Collaboration, "Performance of muon identification in pp collisions at $\sqrt{s} = 7$ TeV", CMS Physics Analysis Summary MUO-10-002, (2010).

[36] CMS Collaboration, "Isolated Photon Reconstruction and Identification at $\sqrt{s} = 7$ TeV", CMS Physics Analysis Summary EGM-10-006, (2010).

[37] CMS Collaboration, "b-Jet Identification in the CMS Experiment", CMS Physics Analysis Summary BTV-11-004, (2012).

[38] CMS Collaboration, "Measurement of btagging efficiency using ttbar events", CMS Physics Analysis Summary BTV-11-003, (2012).

[39] L. Randall and D. Tucker-Smith, "Dijet Searches for Supersymmetry at the Large Hadron Collider", *Phys. Rev. Lett.* **101** (2008) 221803, doi:10.1103/PhysRevLett.101.221803.

[40] CMS Collaboration, "SUSY searches with dijet events", CMS Physics Analysis Summary SUS-08-005, (2008).

[41] CMS Collaboration, "Search strategy for exclusive multi-jet events from supersymmetry at CMS", CMS Physics Analysis Summary SUS-09-001, (2009).

[42] CMS Collaboration, "Data-Driven Estimation of the Invisible Z Background to the SUSY MET Plus Jets Search", CMS Physics Analysis Summary SUS-08-002, (2008).

[43] Z. Bern, G. Diana, L. Dixon et al., "Driving Missing Data at Next-to-Leading Order", *Phys.Rev.* **D84** (2011) 114002, doi:10.1103/PhysRevD.84.114002, arXiv:1106.1423.